CELL REGULATION, Vol. 1, 99–112, November 1989

Mitogen-induced oscillations of cytosolic Ca^{2+} and transmembrane Ca^{2+} current in human leukemic T cells

Richard S. Lewis and Michael D. Cahalan
Department of Physiology and Biophysics
California College of Medicine
University of California, Irvine
Irvine, California 92717

A rapid rise in the level of cytosolic free calcium ($[Ca^{2+}]_i$) is believed to be one of several early triggering signals in the activation of T lymphocytes by antigen. Although Ca^{2+} release from intracellular stores and its contribution to Ca^{2+} signaling in many cell types is well documented, relatively little is known regarding the role and mechanism of Ca^{2+} entry across the plasma membrane. We have investigated mitogen-triggered Ca^{2+} signaling in individual cells of the human T-leukemia-derived line, Jurkat, using fura-2 imaging and patch-clamp recording techniques. Phytohemagglutinin (PHA), a mitogenic lectin, induces repetitive $[Ca^{2+}]_i$ oscillations in these cells peaking at micromolar levels with a period of 90–120 s. The oscillations depend critically upon Ca^{2+} influx across the plasma membrane, as they are rapidly terminated by removal of extracellular Ca^{2+}, addition of Ca^{2+}-channel blockers such as Ni^{2+} or Cd^{2+}, or membrane depolarization. Whole-cell and perforated-patch recording methods were combined with fura-2 measurements to identify the mitogen-activated Ca^{2+} conductance involved in this response. A small, highly selective Ca^{2+} conductance becomes activated spontaneously in whole-cell recordings and in response to PHA in perforated-patch experiments. This conductance has properties consistent with a role in T-cell activation, including activation by PHA, lack of voltage-dependent gating, inhibition by Ni^{2+} or Cd^{2+}, and regulation by intracellular Ca^{2+}. Moreover, a tight temporal correlation between oscillations of Ca^{2+} conductance and $[Ca^{2+}]_i$ suggests a role for the membrane Ca^{2+} conductance in generating $[Ca^{2+}]_i$ oscillations in activated T cells.

Introduction

The specific binding of antigen and associated major histocompatibility proteins by the T-cell receptor complex initiates the activation of T lymphocytes in vivo. The activation process comprises a spectrum of cellular changes: the receptor for interleukin-2 is expressed, helper T cells are stimulated to synthesize and secrete lymphokines, cytotoxic T cells acquire the ability to kill foreign target cells, and T cells of all classes progress from G_0 through the cell cycle, eventually undergoing DNA replication and mitosis. Some or all of these cellular changes can be induced in vitro by treatment with phorbol esters together with antibodies that crosslink selected surface glycoproteins, such as the T-cell receptor, CD3, and CD2 molecules, or with mitogenic lectins such as phytohemagglutinin (PHA)[1] or concanavalin A (for reviews, see MacDonald and Nabholz, 1986; Weiss and Imboden, 1987).

Among the earliest activation events in many cell types, including lymphocytes, are the hydrolysis of phosphatidylinositol 4,5-bisphosphate (PIP_2) and a rise in the level of cytosolic free Ca^{2+} (Berridge and Irvine, 1984). The cytosolic free calcium ($[Ca^{2+}]_i$) rise is believed to be an important triggering signal for T-cell activation, based on several lines of indirect evidence. First, many polyclonal T-cell activators, as well as specific antigens, evoke a rise in $[Ca^{2+}]_i$ (Tsien *et al.*, 1982; Nisbet-Brown *et al.*, 1985; Imboden and Stobo, 1985; Oettgen *et al.*, 1985; Treves *et al.*, 1987). In these cases, blocking the rise pharmacologically or by removing extracellular Ca^{2+} inhibits proliferation and other activation events (Whitney and Sutherland, 1972; M. Weiss *et al.*, 1984; Gelfand *et al.*, 1986). In addition, artificial elevation of intracellular $[Ca^{2+}]$ using ionophores, in the presence of phorbol esters to activate protein kinase C, bypasses the involvement of cell-surface receptors and activates T cells (Mastro and Smith, 1983; Weiss *et al.*, 1984; Truneh *et al.*, 1985).

Measurements of $[Ca^{2+}]_i$ in single cells using the Ca^{2+}-sensitive dye fura-2 (Grynkiewicz *et al.*, 1985) or the photoprotein aequorin have revealed several surprising features of intracellular Ca^{2+} dynamics previously undetectable in cell suspensions; e.g., activation of a range of cells, including cytotoxic T lymphocytes (Gray *et al.*, 1988), B lymphocytes (Wilson *et al.*, 1987), mast cells

[1] Abbreviations: IP_3, inositol 1,4,5-trisphosphate; PHA, phytohemagglutinin-P; PIP_2, phosphatidylinositol 4,5-bisphosphate.

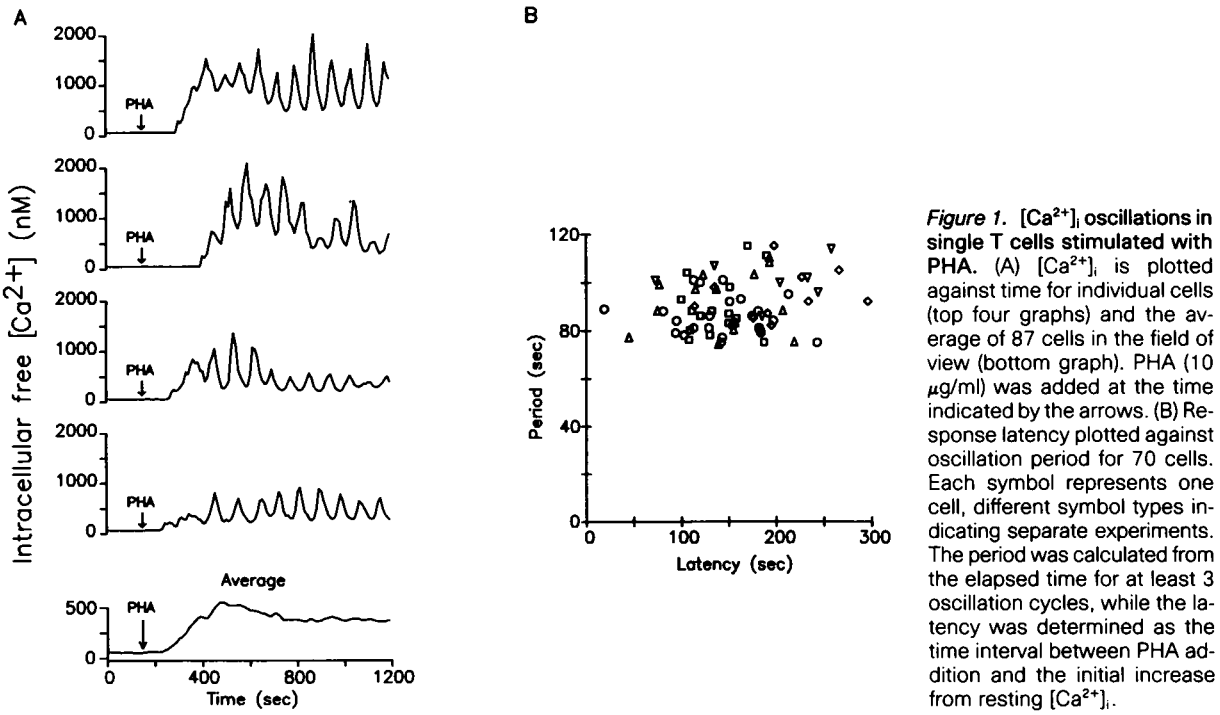

Figure 1. **$[Ca^{2+}]_i$ oscillations in single T cells stimulated with PHA.** (A) $[Ca^{2+}]_i$ is plotted against time for individual cells (top four graphs) and the average of 87 cells in the field of view (bottom graph). PHA (10 μg/ml) was added at the time indicated by the arrows. (B) Response latency plotted against oscillation period for 70 cells. Each symbol represents one cell, different symbol types indicating separate experiments. The period was calculated from the elapsed time for at least 3 oscillation cycles, while the latency was determined as the time interval between PHA addition and the initial increase from resting $[Ca^{2+}]_i$.

(Neher and Almers, 1986), hepatocytes (Woods *et al.*, 1987), vascular endothelial cells (Jacob *et al.*, 1988), and oocytes (Cuthbertson and Cobbold, 1985; Miyazaki *et al.*, 1986) elicits repetitive $[Ca^{2+}]_i$ oscillations (for review, see Berridge *et al.*, 1988). The mechanisms underlying these oscillations have not yet been firmly established, but are believed to involve the repetitive release and reuptake of Ca^{2+} from intracellular storage sites such as the endoplasmic reticulum, with Ca^{2+} influx across the plasma membrane serving only to replenish the stores (Woods *et al.*, 1987; Berridge *et al.*, 1988; Meyer and Stryer, 1988; Payne *et al.*, 1988). While inositol 1,4,5-trisphosphate (IP_3) is known to release Ca^{2+} from internal stores (Streb *et al.*, 1983; Imboden and Stobo, 1985; Meyer *et al.*, 1988), and specific IP_3 receptors have been purified (Supattapone *et al.*, 1988), considerably less is known about the characteristics of the Ca^{2+} influx pathway. Ca^{2+}-permeable channels activated by mitogens and IP_3 have been reported in the plasma membrane of T cells, but their degree of Ca^{2+} permeability and, hence, their contribution to Ca^{2+} signaling during T-cell activation has not been assessed (Kuno *et al.*, 1986; Kuno and Gardner, 1987).

We have used fura-2 fluorescence-ratio imaging to characterize $[Ca^{2+}]_i$ oscillations induced by PHA in Jurkat T cells, with the primary aim of identifying a current component corresponding to Ca^{2+} influx. In this paper we initially characterize the ionic dependence of Ca^{2+} signals in individual cells using video-imaging techniques. Based on these results, electrophysiological methods are used to identify a membrane Ca^{2+} conductance with properties consistent with those of the mitogen-activated Ca^{2+} influx pathway. Simultaneous measurement and correlation of $[Ca^{2+}]_i$ and membrane current in single cells confirms an important role for this conductance in mediating Ca^{2+} influx in response to mitogenic stimulation. A preliminary report of this work has appeared (Lewis and Cahalan, 1989).

Results

PHA induces oscillations of intracellular $[Ca^{2+}]$

We examined the changes in free $[Ca^{2+}]_i$ induced by PHA treatment in individual Jurkat cells through fluorescence-ratio imaging of cells loaded with fura-2. Treatment of Jurkat cells with PHA (10 μg/ml) elicited a rise in $[Ca^{2+}]_i$ from the resting level of 116 ± 48 nM to a peak of 518 ± 149 nM (mean ± SD in 18 experiments) after a relatively long and variable delay (Figure 1A). In the majority of cases the initial rising phase was quite abrupt, reaching a peak within 5–10 s. Thereafter, $[Ca^{2+}]_i$ often began to oscillate slowly, reaching peak levels in the micromolar range. The average period of the oscillations was 92 ± 12 s (62 cells; mean ± SD), while the response delay was 174 ± 63 s (119 cells; mean ± SD). The oscillation period among

cells was more narrowly distributed than the response delay, and the two parameters showed no significant correlation (Figure 1B). This finding suggests independence between the rate-limiting step for initiating the Ca^{2+} response and the process that determines the oscillation period. About 90% of the cells tested responded to PHA, and 80% of these produced multiple $[Ca^{2+}]_i$ oscillations during the 20-min test period.

Because oscillations in single cells are not synchronous, the average response of 87 cells appears smooth (Figure 1A, bottom trace). The average response has both a "transient" and "sustained" phase, much like the population response of Jurkat cell suspensions (Imboden and Stobo, 1985). The results shown here indicate that the sustained phase of the $[Ca^{2+}]_i$ rise identified in cell suspensions actually results from asynchronous $[Ca^{2+}]_i$ oscillations at the single-cell level.

Ca^{2+} influx is required for $[Ca^{2+}]_i$ oscillations

Several lines of evidence suggest that Ca^{2+} influx across the plasma membrane is required to both initiate and sustain $[Ca^{2+}]_i$ oscillations. First, PHA does not induce oscillations when added in the presence of a low level (5 μM) of extracellular Ca^{2+}, although small, infrequent $[Ca^{2+}]_i$ transients occur, presumably due to release from intracellular stores (Lewis and Cahalan, 1989). Extracellular Ca^{2+} is also necessary to maintain the oscillations, since reducing $[Ca^{2+}]_o$ to 5 μM after initiation of the response in normal $[Ca^{2+}]_o$ rapidly and reversibly terminates the oscillations (Figure 2A). The extreme sensitivity of $[Ca^{2+}]_i$ oscillations in Jurkat cells to reduction of extracellular $[Ca^{2+}]$ suggests that they depend critically on influx (see Discussion).

Active feedback control of intracellular $[Ca^{2+}]$ is indicated by the overshoot occurring upon restoration of 2 mM Ca^{2+} to activated cells bathed in low-Ca^{2+} medium (Figure 2A). Likewise, elevating extracellular $[Ca^{2+}]$ to 10 mM evokes only a transient increase in the average $[Ca^{2+}]_i$ (Figure 2B). These results may reflect Ca^{2+}-dependent stimulation of the plasmalemma Ca^{2+}-ATPase as well as Ca^{2+}-induced inhibition of the influx pathway (discussed below).

A role for Ca^{2+} influx in sustaining the oscillations is also supported by the inhibitory effects of membrane depolarization or exposure to Ca^{2+}-channel blocking ions. Substitution of K^+ for all Na^+ in the normal Ringer solution effectively and reversibly suppresses the PHA-evoked Ca^{2+} rise (Figure 3A), while replacement of Na^+ with choline or tetramethylammonium does not (data not shown). As high $[K^+]_o$ is known to depolarize the T-cell membrane (Gelfand *et al.*, 1984), its effect on $[Ca^{2+}]_i$ may be explained largely by a reduction in the inwardly directed electrical driving force on Ca^{2+}. However, additional effects of depolarization or high $[K^+]_o$ itself on Ca^{2+} efflux via the membrane Ca^{2+}-ATPase cannot be ruled out (Ishida and Chused, 1988). As noted previously by others (Gelfand *et al.*, 1984; Oettgen *et al.*, 1985), the fact that high $[K^+]_o$ alone does not elevate $[Ca^{2+}]_i$ indicates that T cells do not express voltage-dependent Ca^{2+} channels common to electrically excitable cells. This conclusion is also supported

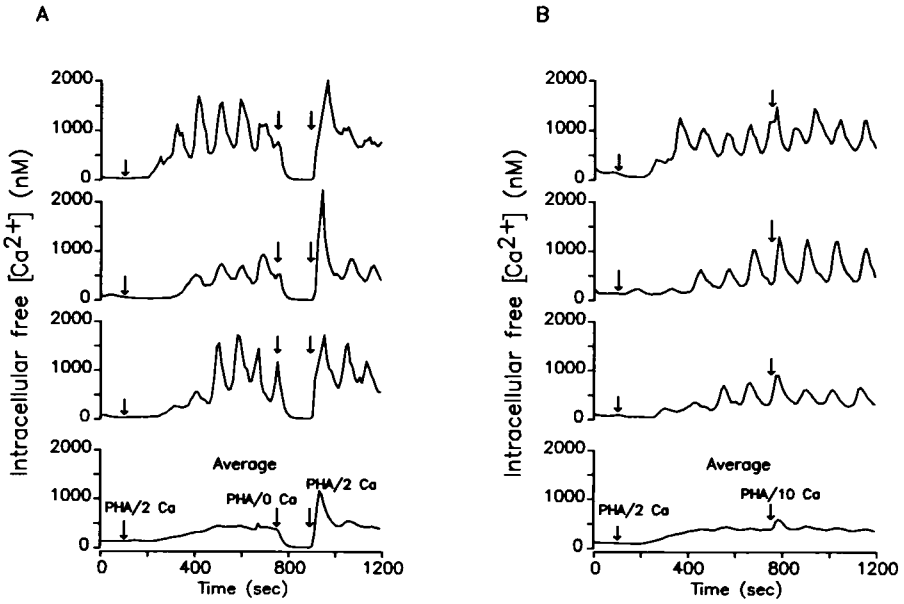

Figure 2. **Dependence of $[Ca^{2+}]_i$ oscillations on extracellular Ca^{2+}.** In (A) and (B), the top three graphs represent single cells, and the bottom graph is the average of >70 cells from the same experiment. (A) Effect of low $[Ca^{2+}]_o$ on the PHA-evoked response. Cells were exposed to PHA (10 μg/ml) in Ringer (containing 2 mM Ca^{2+}), then to PHA in nominally Ca^{2+}-free Ringer (containing 5 μM Ca^{2+}) followed by a return to normal $[Ca^{2+}]_o$. (B) Effect of $[Ca^{2+}]_o$ elevation on the $[Ca^{2+}]_i$ oscillations. Cells were exposed sequentially to PHA (10 μg/ml) in 2 mM Ca^{2+} and in 10 mM Ca^{2+}.

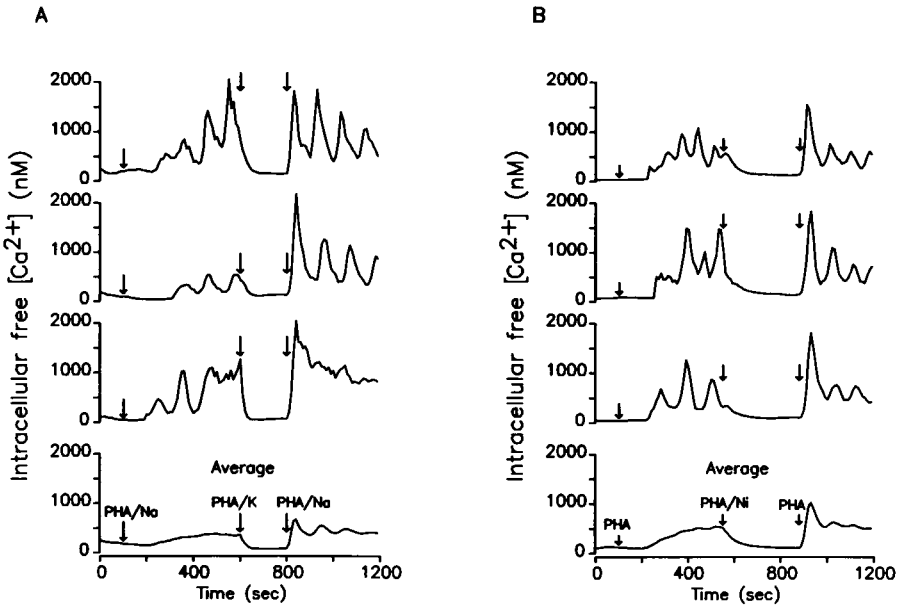

Figure 3. **Block of PHA-stimulated $[Ca^{2+}]_i$ oscillations by high extracellular $[K^+]$ or Ni^{2+}.** In (A) and (B), the top three graphs represent single cells, and the bottom graph is the average of >70 cells from the same experiment. (A) After initiating the response to PHA (10 μg/ml) in Ringer solution, extracellular Na^+ was replaced with K^+, then returned to the bath. Oscillatory activity in the average response is enhanced upon return to normal Ringer, reflecting synchronization of cells as well as enhanced peak-to-peak oscillation amplitude. (B) 5 mM Ni^{2+} blocks the PHA-evoked $[Ca^{2+}]_i$ rise reversibly.

by a failure to detect voltage-dependent Ca^{2+} conductance using patch-clamp methods (Fukushima *et al.*, 1984; Matteson and Deutsch, 1984; Cahalan *et al.*, 1985). The $[Ca^{2+}]_i$ rise is largely blocked by 5 mM Ni^{2+} (Figure 3B) and 1 mM Cd^{2+} (data not shown), divalent cations known to block Ca^{2+} channels in a variety of preparations (for review, see Hagiwara and Byerly, 1981).

In summary, the Ca^{2+}-imaging results suggest that oscillations result from Ca^{2+} influx through a Ni^{2+}- and Cd^{2+}-sensitive transport mechanism that is not activated by depolarization, yet is electrogenic (i.e., carries net charge across the membrane), as depolarization inhibits influx. These findings place important constraints on the properties of the PHA-activated Ca^{2+} influx pathway. To identify and characterize this pathway more directly, single-cell Ca^{2+} measurements were subsequently combined with simultaneous electrical recording using the whole-cell patch-clamp technique.

Ca^{2+} conductance activates spontaneously during whole-cell patch-clamp recording

In conventional whole-cell recording (Hamill *et al.*, 1981), a polished glass micropipette is first sealed to the cell membrane, after which the patch of membrane beneath the pipette lumen is ruptured by negative pressure applied to the pipette's interior. The rupture of the patch, which we will refer to hereafter as "break-in," provides electrical access to the cell's interior necessary for whole-cell recording while initiating dialysis of the cytoplasm by the pipette contents. In >80% of the Jurkat cells studied, a Ca^{2+}-selective conductance became activated within seconds to several minutes of break-in, possibly due to disruption of the cell's normal cytoplasmic constituents by internal dialysis. Although the Ca^{2+} conductance appeared in the absence of PHA, its properties were consistent with those of the PHA-activated Ca^{2+} transport pathway described above, and in many cases its activity during whole-cell recording was stable for several minutes or more, thus facilitating its characterization.

Spontaneous activation of Ca^{2+} influx during whole-cell recording is illustrated in Figure 4. In this experiment, we applied a staircase command voltage (Figure 4A, top trace) to the membrane to assess the degree to which intracellular $[Ca^{2+}]$ was sensitive to membrane potential. Simultaneously, the membrane current (Figure 4A, middle trace) and intracellular $[Ca^{2+}]$ (Figure 4A, bottom trace) were measured. Shortly after break-in, $[Ca^{2+}]_i$ rose to a peak of >1 μM, then returned slowly to its resting level of 100 nM. Superimposed on the response are rapid $[Ca^{2+}]_i$ fluctuations driven by the imposed changes in membrane potential. The ability of the membrane potential to modulate intracellular $[Ca^{2+}]$ suggests that Ca^{2+} influx contributes to the spontaneous $[Ca^{2+}]_i$ rise. The enlarged view of Figure 4B shows that membrane depolarization reduces $[Ca^{2+}]_i$ while hyperpolarization enhances it. This result is similar to the effect of K^+-induced depolarization on Ca^{2+} signaling in intact cells (Figure 3A) and may be explained by depolarization reducing the electrical driving force for Ca^{2+} entry.

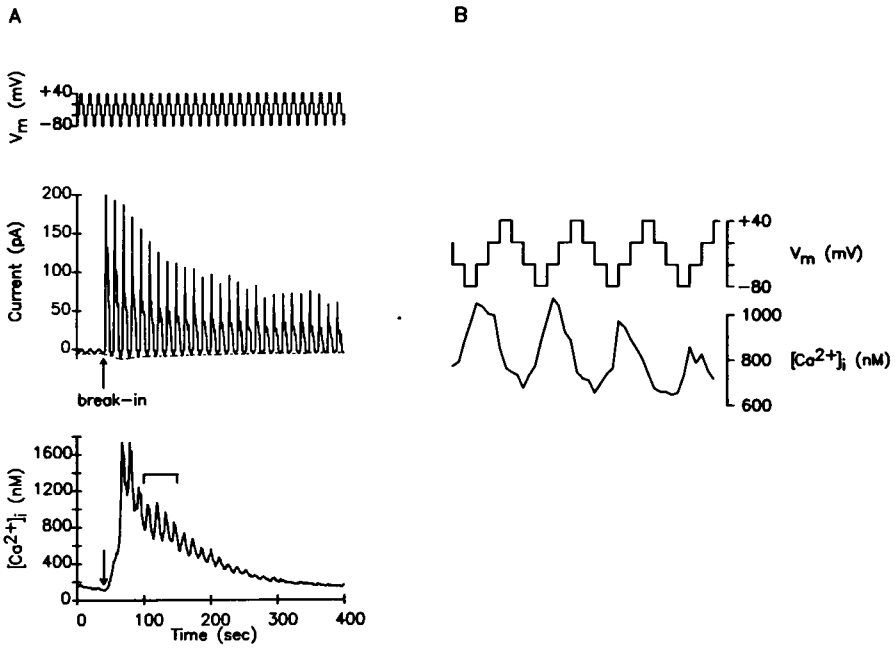

Figure 4. **Spontaneous increase in intracellular $[Ca^{2+}]$ and activation of ionic currents during whole-cell recording.** (A) The command potential (V_m) was held for 2 s at −80 to +40 mV in 40-mV increments (top) as membrane current (middle) and $[Ca^{2+}]_i$ (bottom) were measured. "Break-in" to the whole-cell recording configuration is indicated by the arrows. Voltage-gated K^+ channels are activated by depolarization above −40 mV, giving rise to the positive current spikes that slowly decline in size as the channels accumulate inactivation. In addition, a transient inward current prominent at −80 mV (dashed line) is correlated with the overall time course of $[Ca^{2+}]_i$. In this experiment, the internal (pipette) solution lacked EGTA. (B) Expanded view of $[Ca^{2+}]_i$ and membrane potential (V_m) from the bracketed time period in A. Depolarization suppresses and hyperpolarization elevates $[Ca^{2+}]_i$.

Several types of ionic conductances are activated during the experiment illustrated in Figure 4. Voltage-gated K^+ channels, activated by depolarization, produce the large positive current transients in Figure 4A (DeCoursey *et al.*, 1984; Matteson and Deutsch, 1984; Fukushima *et al.*, 1984; Cahalan *et al.*, 1985). In addition, a small inward current develops at a membrane potential of −80 mV, as indicated by the dashed line. The time course of this current parallels that of the $[Ca^{2+}]_i$ rise; this characteristic and other properties described below identify it as a selective Ca^{2+} current which is responsible for the spontaneous rise in cytosolic $[Ca^{2+}]$. Interestingly, the Ca^{2+} current often developed during whole-cell recordings without a detectable increase in current noise, implying a very small unitary conductance for the Ca^{2+} transport mechanism. A third conductance, detectable as a small outward current at −40 mV, results from Ca^{2+}-dependent K^+ channels activated by the increase in $[Ca^{2+}]_i$ (Grissmer and Cahalan, 1989; Schlichter and Mahaut-Smith, 1989; R. Lewis, S. Grissmer, and M. Cahalan, unpublished observations). At its reversal potential of −80 mV, however, the Ca^{2+}-activated K^+ current is absent and thus does not interfere with measurement of the Ca^{2+} current.

In experiments like that shown in Figure 4, performed with pipette (internal) solutions of low Ca^{2+}-buffering strength (100 μM fura-2 being the only Ca^{2+} buffer present), the peak inward Ca^{2+} current tended to be quite small, −2.8 ± 1.9 pA (mean ± SD) measured at −80 mV (n = 7 cells). In most experiments, 10 mM EGTA was included in the pipette solution. In addition to prolonging the Ca^{2+} current, intracellular EGTA enhanced its amplitude to an average of −6.6 ± 3.2 pA (mean ± SD, n = 20 cells) and prevented activation of the Ca^{2+}-activated K^+ current by clamping $[Ca^{2+}]_i$ to a low value, thereby facilitating characterization of the Ca^{2+} current. The augmentation of Ca^{2+} current by intracellular Ca^{2+} buffering is consistent with previous reports (Kuno and Gardner, 1987; MacDougall *et al.*, 1988) and our own indirect observations (Figure 2B) that intracellular Ca^{2+} negatively regulates Ca^{2+} conductance in lymphocytes.

Properties of the calcium conductance

Ionic substitution experiments show that under physiological conditions the slowly developing inward current is carried primarily by Ca^{2+}. In these experiments, membrane current was recorded

over a range of potentials as voltage ramps were applied to the cell (Figures 5–7). With physiological concentrations of intra- and extracellular ions, the current is inwardly directed at potentials as positive as −30 mV (Figure 6); because the equilibrium potential for K^+ and Cl^- is −95 mV under these conditions, this result indicates negligible permeability to these ions. In the experiment shown in Figure 5, intracellular Cs^+ and extracellular tetrodotoxin were used to block current through voltage-gated K^+ and Na^+ channels, respectively, thus isolating the Ca^{2+} current. Under these conditions, the current is inward at potentials as positive as +20 mV, and does not reverse sign at potentials up to +100 mV. The inward Ca^{2+} current declines as the membrane potential is made more positive, indicating that, unlike the Ca^{2+} channels of excitable cells, the T cell's Ca^{2+} transporter is not activated by depolarization. Prolonged depolarization also does not inhibit the conductance; instead, the decrease in Ca^{2+} current at depolarized potentials, like the reduction in Ca^{2+} influx under comparable conditions (Figures 3A and 4B), is explained most simply by a reduction in the driving force on Ca^{2+}.

The current's selectivity for Ca^{2+} over Na^+ is shown by its dependence upon extracellular Ca^{2+}. As expected for a current carried by Ca^{2+}, it is substantially diminished by reduction of $[Ca^{2+}]_o$ to 5 μM (Figure 6A); in 6 cells, current was on average reduced to 13% of its control value. In contrast, complete replacement of extracellular

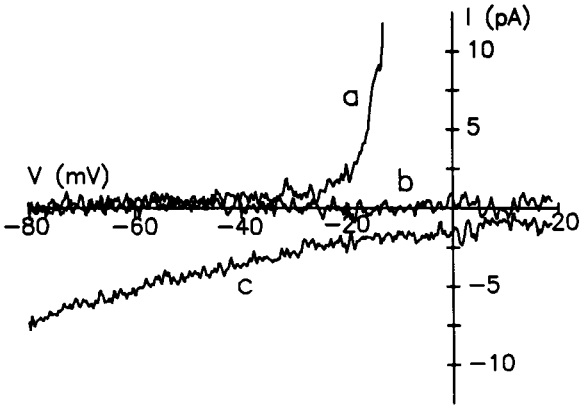

Figure 5. **Ca^{2+} and K^+ currents in Jurkat cells.** Membrane potential, V, was varied from −80 mV to +20 mV over a 200-ms period as membrane current, I, was recorded. Currents were collected 1 s (a), 14 s (b), and 60 s (c) after break-in with Cs aspartate internal (pipette) solution. Voltage-gated K^+ channels are open at voltages positive to −30 mV early in the recording, producing outward current (a). Over the first 15 s, Cs^+ in the recording pipette diffuses into the cell and blocks this current (b). After 1 min, a Ca^{2+} current develops that is inwardly directed at potentials up to +20 mV (c).

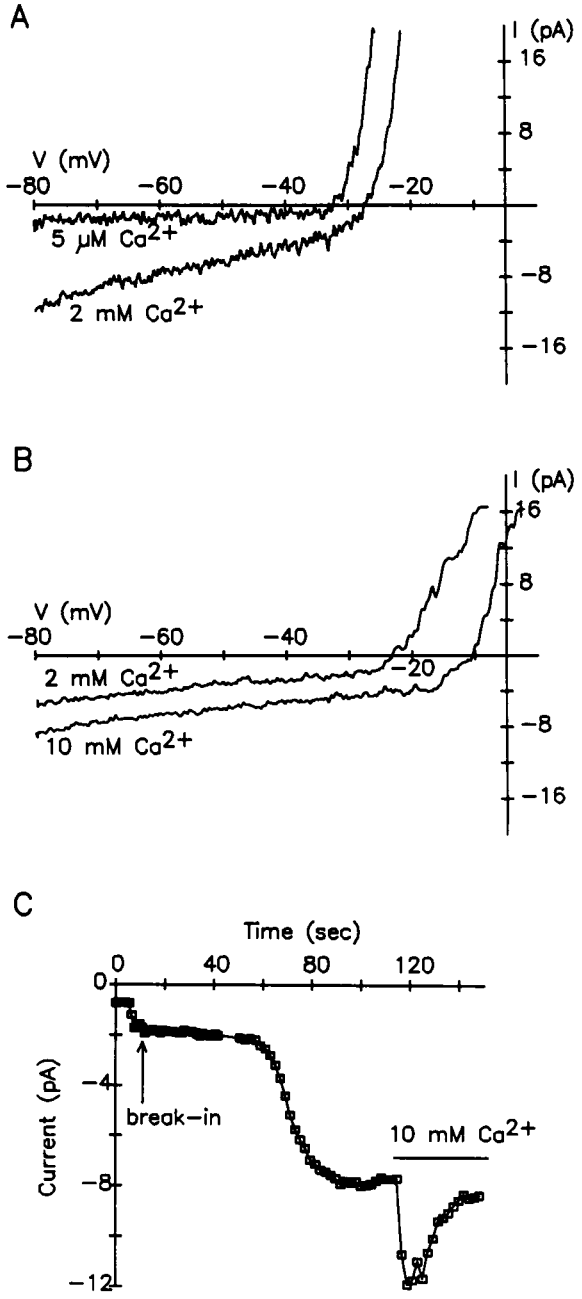

Figure 6. **Selectivity and regulation of the Ca^{2+} current.** Voltage stimuli were delivered and currents recorded as in Figure 5, but with a pipette solution containing K aspartate. (A) Dependence of inward current on extracellular Ca^{2+}. Lowering $[Ca^{2+}]_o$ to 5 μM reduces the inward current to 10% of its control amplitude (in 2 mM Ca^{2+}) and shifts the voltage dependence of K^+-channel activation to more negative potentials. These effects were reversible (not shown). (B) Enhancement of inward current by elevating $[Ca^{2+}]_o$. Shortly after perfusion with Ringer containing 10 mM Ca^{2+}, the inward current is increased and the extrapolated reversal potential shifts to the right. In addition, the voltage dependence of K^+-channel activity is shifted to more positive potentials. (C) A plot of current at −80 mV against time for the experiment of (B) shows that the increase in Ca^{2+} current is transient.

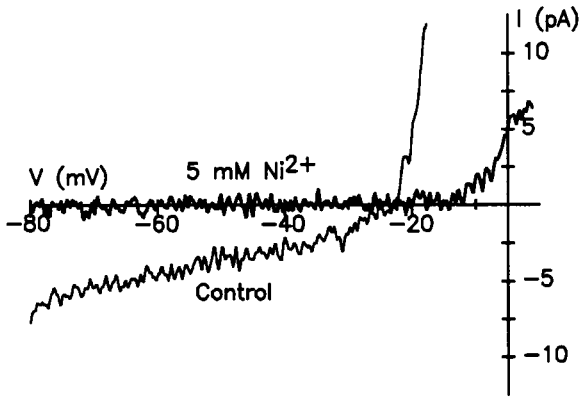

Figure 7. **Block of Ca^{2+} current by extracellular Ni^{2+}.** Application of 5 mM Ni^{2+} (bold trace) completely inhibits the inward current and partially blocks and alters the voltage dependence of voltage-gated K^+ channels. The block of Ca^{2+} current in this experiment was 80% reversible. Recording conditions as in Figure 6.

Na^+ with the relatively large, impermeant cations choline or tetramethylammonium, had a less pronounced effect, reducing the inward current to 50–60% of control. Elevating $[Ca^{2+}]_o$ from 2 to 10 mM markedly enhances the size of the inward current and shifts its extrapolated reversal potential to more positive voltages, again reflecting a significant permeability to Ca^{2+} (Figure 6B). Interestingly, this increase in current is transient; in the continued presence of 10 mM Ca^{2+} the current returns over a period of ~30 s to the level recorded in 2 mM Ca^{2+} (Figure 6C). This result is consistent with regulation of the Ca^{2+} conductance by $[Ca^{2+}]_i$ (see Discussion). Finally, the current is blocked reversibly by application of 5 mM Ni^{2+} (Figure 7) or 1 mM Cd^{2+} to the bathing medium.

In summary, the inward current appearing spontaneously during whole-cell recording has properties suggesting its involvement in PHA-stimulated Ca^{2+} signaling in Jurkat cells. It is selective for Ca^{2+} over Na^+, K^+, and Cl^-, and is blocked by Ni^{2+} and Cd^{2+} at concentrations that block the $[Ca^{2+}]_i$ rise in PHA-stimulated cells. The inward current also declines with depolarization (Figure 5), consistent with the inhibition of Ca^{2+} signaling in intact cells by high $[K^+]_o$ (Figure 3A). To establish more firmly the physiological function of this current, however, requires a test of whether it can be induced by PHA. Clearly, this point cannot be addressed with conventional whole-cell recording methods, as the current appears spontaneously in the absence of mitogen, presumably due to dialysis of the cell cytoplasm by the pipette contents during whole-cell recording. The following section describes experiments using a variation of the whole-cell recording technique that demonstrate activation of the Ca^{2+} conductance by PHA.

PHA activates an oscillatory Ca^{2+} current during perforated-patch recording

To prevent disruption of the cytosol during recording, we applied the perforated-patch technique using recording pipettes filled with a solution containing nystatin, a pore-forming antibiotic (Horn and Marty, 1988). After formation of the pipette-membrane seal, nystatin spontaneously inserts into the patch beneath the pipette lumen. The resulting nystatin channels provide the necessary electrical connection between the pipette and the cell's interior, without permitting loss of intracellular constituents such as divalent cations and organic molecules.

In perforated-patch experiments, PHA evoked a $[Ca^{2+}]_i$ rise in Jurkat cells that was accompanied by a transient inward current of peak amplitude 0.5–1 pA at −80 mV (data not shown). In some cases the response was oscillatory, fluctuations of inward current being associated with changes in $[Ca^{2+}]_i$. As in the whole-cell experiments described above, intracellular Ca^{2+} buffers appeared to augment the size of the current and thus facilitate its measurement. Therefore, cells in most experiments were preloaded with the Ca^{2+} chelator, BAPTA, in addition to fura-2. As illustrated in Figure 8A, PHA induced delayed, damped $[Ca^{2+}]_i$ oscillations in BAPTA-loaded cells. Corresponding closely to each fluctuation in $[Ca^{2+}]_i$ is a transient increase in inward current. One $[Ca^{2+}]_i$ oscillation and the associated current have been superimposed on a normalized scale in Figure 8B to highlight the causal role of the current in generating the $[Ca^{2+}]_i$ change. The rise and fall of the current precede the rise and fall of $[Ca^{2+}]_i$, as would be expected for a transient Ca^{2+} current flowing into a buffered compartment. The nonlinear shape of the current in ramp recordings (similar to that in Figure 6), its inhibition by extracellular Ca^{2+} removal or 5 mM Ni^{2+} (data not shown), and the lack of detectable current noise as it activates indicate that the PHA-activated inward current is identical to the Ca^{2+} current appearing spontaneously during whole-cell recording. Taken together with the Ca^{2+}-imaging experiments described above, the perforated-patch results suggest that oscillations in intracellular $[Ca^{2+}]$ induced by PHA result from a slowly fluctuating Ca^{2+} conductance in the plasma membrane.

Discussion

In this study, we have demonstrated that the mitogenic lectin, PHA, elicits repetitive $[Ca^{2+}]_i$ os-

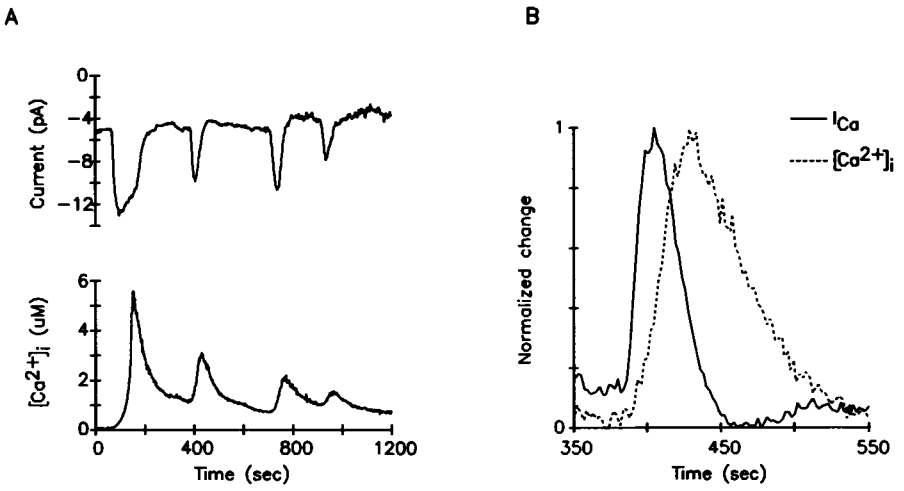

Figure 8. **Oscillations in $[Ca^{2+}]_i$ and Ca^{2+} current evoked by PHA during "perforated-patch" recording.** The cell was pre-loaded with BAPTA and fura-2. (A) PHA (10 μg/ml) added at time 0 induces repetitive $[Ca^{2+}]_i$ oscillations (lower graph), each of which is accompanied by a transient of inward current measured at −80 mV (upper graph). (B) Change in current (solid line) and $[Ca^{2+}]_i$ (dashed line) plotted on a normalized scale against time for the second oscillation in (A). The rise and fall of Ca^{2+} current precede the changes in $[Ca^{2+}]_i$, implying that the current is a cause, rather than a consequence, of the rise in intracellular $[Ca^{2+}]$.

cillations in Jurkat T cells that are critically dependent on Ca^{2+} influx across the plasma membrane. Simultaneous measurement of $[Ca^{2+}]_i$ and membrane current has made it possible for the first time to identify the Ca^{2+} conductance responsible for driving the oscillations. The salient features of the conductance include activation by PHA, cyclic activation and deactivation preceding the rise and fall of intracellular $[Ca^{2+}]$, respectively, a high selectivity for Ca^{2+} over other ions, a very low unitary conductance, and an apparent lack of voltage-dependent gating.

Ca^{2+} measurements in single cells and cell suspensions

The use of video-imaging techniques to study mitogen-activated Ca^{2+} signaling at the level of individual T lymphocytes reveals a level of complexity in cellular responses not detectable in cell suspensions. Spectrofluorimetric measurements on suspensions of cells using Ca^{2+}-sensitive dyes have shown that mitogens or other stimuli triggering the hydrolysis of PIP_2 elicit a biphasic $[Ca^{2+}]_i$ increase. Examples include mitogenic lectins and monoclonal antibodies to CD2, CD3, and T-cell receptor molecules for T cells (Hesketh *et al.*, 1985; Imboden and Stobo, 1985; June *et al.*, 1986), and anti-Ig treatment of B lymphocytes (Bijsterbosch *et al.*, 1986). Activation of platelets (Hallam and Rink, 1985), hepatocytes (Williamson *et al.*, 1985), and parotid gland cells (Merritt and Rink, 1987) is also accompanied by a biphasic increase in $[Ca^{2+}]_i$. The common consensus of these studies has been that the initial transient phase of the response arises from internal Ca^{2+} release triggered by IP_3, while the later, sustained phase depends upon Ca^{2+} influx across the plasma membrane. From single-cell imaging experiments it is now clear that the sustained phase of the average response in a T-cell population actually derives from pronounced $[Ca^{2+}]_i$ oscillations triggered in individual cells by PHA (Figure 1A). The oscillations occur asynchronously and therefore tend to become obscured in the sum of a large number of cells. Similar observations have been reported for individual B cells stimulated with antibodies to surface immunoglobulin molecules (Wilson *et al.*, 1987). The character of single-cell responses may have important implications for the elucidation of underlying molecular mechanisms. For example, one important caveat inherent to suspension measurements is that they may seriously underestimate peak cellular Ca^{2+} levels (Figures 1–3). Knowledge of these peak values may ultimately facilitate the identification of intracellular Ca^{2+}-sensitive effector proteins that are involved in T-cell activation. In addition, the oscillatory pattern of $[Ca^{2+}]_i$ fluctuations per se may be an essential element of the signaling process, as discussed below. The lack of correlation between response latency and oscillation period for single cells (Figure 1B) implies that these two response parameters may be used to probe independent intracellular events, latency being an indicator of events preceding the initial response (such as the accumulation of a threshold level of intracellular messenger), and period being an in-

dicator of feedback involved in generating oscillations.

$[Ca^{2+}]_i$ oscillations depend upon Ca^{2+} influx

The sensitivity of $[Ca^{2+}]_i$ oscillations in single T cells to low $[Ca^{2+}]_o$, high $[K^+]_o$, and extracellular Ni^{2+} and Cd^{2+} implies a direct dependence on Ca^{2+} influx across the plasma membrane. These results confirm and extend earlier studies showing that EGTA blocks the sustained $[Ca^{2+}]_i$ rise in suspensions of stimulated Jurkat cells or thymocytes (Imboden and Stobo, 1985; Hesketh *et al.*, 1985). Depolarization by high $[K^+]_o$ also inhibits mitogen-induced $[Ca^{2+}]_i$ signals in suspensions of human T cells (Gelfand *et al.*, 1984) and HPB-ALL tumor T cells (Oettgen *et al.*, 1985). Millimolar levels of Ni^{2+}, similar to those we found to block Ca^{2+} flux in Jurkat cells, block agonist-induced Ca^{2+} influx in nonexcitable cells such as platelets (Hallam and Rink, 1985; Zschauer *et al.*, 1988), mast cells (Matthews *et al.*, 1989), and parotid acinar cells (Merritt and Rink, 1987). The fundamental difference between $[Ca^{2+}]_i$ oscillations in Jurkat cells and those in a variety of other activated cells concerns the degree of dependence on extracellular Ca^{2+}. This difference is discussed in greater detail below.

Mitogen-activated Ca^{2+} conductance in Jurkat T cells

The whole-cell and perforated-patch recording experiments reported here represent the first direct demonstration of a mitogen-gated, selective Ca^{2+} conductance and its contribution to Ca^{2+} signaling in T lymphocytes. The conductance, which also becomes activated during whole-cell recording in the absence of PHA, has five properties expected of the mitogen-gated Ca^{2+} transporter as characterized by the imaging experiments on intact cells. 1) The conductance is selective for Ca^{2+} over other physiological ions, enabling it to carry significant amounts of Ca^{2+} into the cell. 2) The conductance is not gated by changes in membrane potential although inward current declines with depolarization, consistent with the inhibitory effect of high $[K^+]_o$ on Ca^{2+} signaling by PHA. 3) The conductance shows the same sensitivity to inhibition by extracellular Ni^{2+} and Cd^{2+} as the $[Ca^{2+}]_i$ rise. 4) The Ca^{2+} current increases only transiently during continued exposure to elevated $[Ca^{2+}]_o$, consistent with the transient $[Ca^{2+}]_i$ increase in intact cells under the same conditions. 5) The time course of the inward current is tightly correlated in time with changes in $[Ca^{2+}]_i$, increasing and decreasing slightly before the rise and fall of $[Ca^{2+}]_i$, respectively. The mechanism by which the Ca^{2+} conductance becomes activated during whole-cell recordings appears to result from intracellular dialysis by the contents of the recording pipette, as inward Ca^{2+} current does not develop if the pipette is merely sealed to the cell membrane without rupturing the underlying patch. It is possible that an inhibitory intracellular constituent is lost by diffusion into the pipette during whole-cell recording; alternatively, intracellular dialysis may interact with internal messenger systems or alter homeostatic processes in such a way as to activate the conductance. In perforated-patch experiments, in which the cytosol is relatively unperturbed, development of the Ca^{2+} current requires PHA treatment (Figure 8). The properties of the PHA-activated conductance suggest that it is identical to the conductance appearing spontaneously during whole-cell recording.

The Ca^{2+} current described in this paper is most likely not related to mitogen-activated currents reported previously in T cells and T-cell lines (Kuno *et al.*, 1986; Kuno and Gardner, 1987; Gardner *et al.*, 1989). The whole-cell currents of the earlier studies were comparatively large (−30 to −130 pA at −50 mV), rather nonselective (reversing sign at ~ +20 mV in the presence of external 110 mM $BaCl_2$ and internal 160 mM CsCl), and were blocked reversibly by 1–5 mM Cd^{2+}. Although the Ca^{2+} current we observe is similar in terms of sensitivity to Cd^{2+}, it differs significantly in its high Ca^{2+} selectivity, as indicated by the following characteristics. First, it is inwardly directed under physiological ionic conditions, does not reverse direction at potentials as positive as +100 mV, and is highly dependent on extracellular Ca^{2+} (Figure 6). Most importantly, the high Ca^{2+}-selectivity of the conductance we observe is reflected in its ability to increase $[Ca^{2+}]_i$ in unbuffered cells to micromolar levels while conducting a current on the order of 1 pA, over 100 times less current than reported by Gardner *et al.* (1989). We often observe the slow activation of whole-cell Ca^{2+} current without a detectable increase in current noise, making it unlikely that the current reflects activity of the 7-pS, Ca^{2+}-permeable channels reported previously (Kuno *et al.*, 1986; Kuno and Gardner, 1987; Gardner *et al.*, 1989), which would be expected to produce readily discernible current fluctuations as a result of random opening and closing events. This discrepancy could be explained if the channels' unitary conductance is much reduced in 2 mM Ca^{2+} (our extracellular recording conditions) as compared to 110 mM Ba^{2+} (conditions of the previous studies), although single-channel properties were reported to be

similar under both conditions (Kuno and Gardner, 1987).

The apparent lack of current noise accompanying activation of the Ca^{2+} current has several possible implications for the molecular identity of the transport mechanism. If the transporter is an ion channel, then it must have an extremely small unitary conductance (<1 pS) or exceedingly brief openings, such that opening and closing events are undetectable at the recording bandwidth of 2 kHz. Alternatively, the transporter could represent an electrogenic ion pump or exchange mechanism. Although we cannot distinguish among these possibilities at present, the transport mechanism is not likely to be Na^+/Ca^{2+} exchange, as hyperpolarization increases Ca^{2+} influx (Figure 4B), and substitution of choline or tetramethylammonium for extracellular Na^+ does not inhibit $[Ca^{2+}]_i$ oscillations or abolish the current.

A variety of direct and indirect evidence suggests the presence of a second-messenger-operated, voltage-insensitive Ca^{2+} conductance in other types of cells, including mast cells (Kanner and Metzger, 1984; Penner *et al.*, 1988), B lymphocytes (MacDougall *et al.*, 1988), neutrophils (von Tscharner *et al.*, 1986), platelets (Hallam and Rink, 1985; Zschauer *et al.*, 1988), and lacrimal gland cells (Llano *et al.*, 1987). Whole-cell recording of rat peritoneal mast cells has revealed an agonist-triggered ionic current that bears a close resemblance to the current we observe in T cells (Penner *et al.*, 1988; Matthews *et al.*, 1989). Mast cell agonists like 48/80 or substance P evoke a slowly developing inward current of ~1 pA amplitude highly correlated in time with an increase in $[Ca^{2+}]_i$. The conductance is Ca^{2+}-selective, blocked by 5 mM Ni^{2+}, is voltage insensitive, and develops without a measurable increase in current noise (Matthews *et al.*, 1989), much like the Ca^{2+} current in T lymphocytes described here. Thus, signal transduction in T cells and mast cells, and possibly other nonexcitable cell types, may involve similar Ca^{2+} transport mechanisms.

$[Ca^{2+}]_i$ oscillations from a fluctuating Ca^{2+} current in T cells

$[Ca^{2+}]_i$ oscillations are a common feature of the activation of nonexcitable cells, yet little is known regarding their functional roles or their underlying basis. One proposal, that the frequency of $[Ca^{2+}]_i$ oscillations encodes the strength of agonistic stimuli (Woods *et al.*, 1987; Berridge *et al.*, 1988; Jacob *et al.*, 1988), is supported by the striking relation of oscillation frequency to agonist concentration and the relatively immutable shape of individual $[Ca^{2+}]_i$ transients in hepatocytes (Woods *et al.*, 1987) and endothelial cells (Jacob *et al.*, 1988). $[Ca^{2+}]_i$ transients may provide a means of triggering effector pathways while avoiding the cell damage that would result from tonic elevation of $[Ca^{2+}]_i$ (Berridge *et al.*, 1988). Data available at present do not directly address these possibilities in T cells; regardless of their physiological significance, however, oscillations offer a sensitive assay for probing the positive and negative feedback processes that regulate Ca^{2+} signaling.

All of the oscillation models proposed to date rely upon repetitive release and reuptake of Ca^{2+} from intracellular stores (Woods *et al.*, 1987; Meyer and Stryer, 1988; Payne *et al.*, 1988; Berridge *et al.*, 1988). Regulatory feedback in these models occurs at the level of PIP_2 hydrolysis (Woods *et al.*, 1987; Meyer and Stryer, 1988) or Ca^{2+} release from intracellular organelles (Berridge *et al.*, 1988; Payne *et al.*, 1988). The assumed role of Ca^{2+} influx is to help refill the internal stores, although the exact mechanism by which this occurs remains somewhat obscure. A causative role for intracellular Ca^{2+} release in generating oscillations is indicated directly by the persistence of oscillations for a few cycles after removal of extracellular Ca^{2+} from activated mast cells (Neher and Almers, 1986), B lymphocytes (Wilson *et al.*, 1987), endothelial cells (Jacob *et al.*, 1988), and smooth-muscle-derived BC3H-1 cells (Ambler *et al.*, 1988), and by the insensitivity of oscillations to membrane depolarization in endothelial cells (Jacob *et al.*, 1988). However, several observations suggest that the oscillations in Jurkat cells do not result directly from repetitive intracellular release: 1) Intracellular stores in Jurkat cells appear to be relatively exhausted during the sustained phase of the mitogen-induced $[Ca^{2+}]_i$ rise (Imboden and Weiss, 1987). 2) The oscillations are terminated abruptly upon removal of external Ca^{2+}, elevation of $[K^+]_o$, or addition of Ni^{2+} to the medium (Figures 2 and 3). 3) An oscillatory transmembrane Ca^{2+} current precedes the fluctuations of $[Ca^{2+}]_i$ (Figure 8), suggesting that this current drives the $[Ca^{2+}]_i$ oscillations. This hypothesis gains further support from the parallel sensitivity of $[Ca^{2+}]_i$ oscillations and the Ca^{2+} current to Ni^{2+}. Although quite small, the amplitude of the Ca^{2+} current is more than sufficient to account for the rate of $[Ca^{2+}]_i$ rise during the oscillations. A current of 1-pA amplitude is expected to increase $[Ca^{2+}]_i$ by ~10 μM/s in a 12-μm-diameter cell in the absence of buffering; this exceeds by >100-fold the measured maximum rate of rise of $[Ca^{2+}]_i$ during the oscillations illustrated in Figure 1. From these considerations we ten-

tatively conclude that oscillations in Jurkat cells are driven by a Ca^{2+} conductance in the plasma membrane, and elucidation of the oscillation mechanism will thus rest on a more complete understanding of how this conductance is controlled. The fact that PHA induces $[Ca^{2+}]_i$ oscillations even under voltage-clamp conditions (Figure 8) indicates that changes in membrane potential are not the primary driving signal, although a modulatory effect on the rate of Ca^{2+} influx is likely, as evidenced by the inhibition of oscillations (Figure 3A) and reduction of Ca^{2+} current (Figure 5) by depolarization. Instead, the essential feedback loops generating the oscillations are likely to be biochemical rather than electrical in nature. That Ca^{2+} itself may be involved in feedback is indicated by the spontaneous regulation of $[Ca^{2+}]_i$ and Ca^{2+} current after exposure to elevated $[Ca^{2+}]_o$ (Figures 2B and 6C). Inhibition of mitogen-gated, Ca^{2+}-permeable channels by micromolar levels of intracellular Ca^{2+} is also consistent with these observations (Gardner *et al.*, 1989).

Although the magnitude of the Ca^{2+} current alone is probably sufficient to account for the rate of $[Ca^{2+}]_i$ changes during the oscillations, liberation of Ca^{2+} from internal stores may also contribute to the response. For example, Ca^{2+} influx could serve a "pacemaker" role, bringing $[Ca^{2+}]_i$ to a threshold level that triggers intracellular release (Jacob *et al.*, 1988). It is also conceivable that during the sustained phase of the $[Ca^{2+}]_i$ rise, intracellular stores are physically connected to the plasma membrane, as proposed by Putney (1986). If this were the case, oscillations could result from a repetitive release process, and removal of extracellular Ca^{2+} could terminate the oscillations immediately by rapidly depleting the stores. According to such a model, our measurements of Ca^{2+} current would represent influx from the extracellular medium directly through internal storage compartments to the cytosol. Regardless of the precise relationship between Ca^{2+} influx and internal release, the Ca^{2+} current appears to play a central role in the generation of Ca^{2+} oscillations in Jurkat T cells, and will serve as a focal point for further investigation of Ca^{2+} signaling mechanisms in activated T cells.

Methods

Cells

Jurkat E6-1 cells were maintained in a culture medium of RPMI 1640 supplemented with 1 mM glutamine and 10% heat-inactivated fetal bovine serum, in a humidified, 5% CO_2 atmosphere at 37°C. Cells growing in log phase at a density of $0.4–1.8 \times 10^6$/ml were used in experiments.

Solutions

In most experiments, cells were bathed in normal Ringer solution, containing (in mM) 160 NaCl, 4.5 KCl, 2 $CaCl_2$, 1 $MgCl_2$, 5 *N*-hydroxyethylpiperazine-*N*'-2-ethanesulfonic acid (HEPES), adjusted to pH 7.4 with NaOH, and having an osmolarity of 290–320 mOsm. Ca^{2+}-free Ringer was made by substituting $MgCl_2$ for $CaCl_2$, resulting in a free Ca^{2+} level of 5 μM (measured with a Ca^{2+} electrode; Orion Research, Cambridge, MA). K^+ Ringer was made by substituting KCl for NaCl. Phytohemagglutinin-P (PHA-P; Difco, Detroit, MI) was diluted from a frozen stock solution of 10 mg/ml.

Fluorescence ratio imaging with fura-2

Jurkat cells at a density of 10^6/ml were incubated with 3 μM fura-2/AM and, in some cases, 10 μM BAPTA/AM (both from Molecular Probes, Eugene, OR) in culture medium for 30 min at 37°C, washed several times with medium alone, then kept in the dark at room temperature until use (<4 h). After loading, cells were allowed to settle onto glass coverslip chambers and were washed with Ringer solution several minutes before the start of each experiment. On the stage of an IM-35 inverted microscope (Carl Zeiss, Oberkochen, FRG), cells were illuminated alternately at 345 and 375 nm (slit widths = 12 nm) using a dual-monochromator, xenon arc light source (Deltascan I, Photon Technology International, Princeton, NJ) and an electronic shutter (Vincent Associates, Rochester, NY) to restrict illumination to the time of video sampling. Excitation light was deflected with a 405-nm dichroic mirror through a 40× oil-immersion objective (Zeiss Plan-neofluar, N.A. 0.9). Fluorescence emission was collected through a 510-nm bandpass filter (180-nm bandwidth) with a SIT video camera (Hamamatsu Corp., Bridgewater, NJ) connected to a VideoProbe image processor (ETM Systems, Mission Viejo, CA). Sixteen-frame averages at each wavelength collected every 5–10 s were background-subtracted and divided pixel-by-pixel to yield ratio images which were stored on hard disk for off-line analysis. $[Ca^{2+}]_i$ was estimated for individual cells using the equation

$$[Ca^{2+}]_i = K^* \cdot (R - R_{min})/(R_{max} - R)$$

where K^*, R_{min}, and R_{max} were determined from in vivo dye calibration as described below. Optical filters were purchased from Omega Optical (Brattleboro, VT). All experiments were conducted at 22–26°C.

Fura-2/patch-clamp experiments

Recording electrodes were pulled from Accu-fill 90 Micropets (Becton, Dickinson & Co., Parsippany, NJ), coated with Sylgard (Dow Corning Corp., Midland, MI) near their tips and fire-polished. Pipettes had resistances of 2–7 MΩ when filled with K aspartate internal solution (see below). Voltage-clamp experiments were performed using one of two whole-cell recording configurations. For standard whole-cell recording (Hamill *et al.*, 1981; Cahalan *et al.*, 1985) patch pipettes contained (in mM) 160 K aspartate, 2 $MgCl_2$, 10 HEPES, 0.1 fura-2, and 10 K_2 EGTA, adjusted to pH 7.2 with KOH. Cs aspartate internal solution was prepared in the same way, replacing K^+ with Cs^+. In some experiments, EGTA was omitted from the pipette solution to minimize effects on resting $[Ca^{2+}]_i$ or the endogenous buffering capacity of the cell. Under these conditions, free $[Ca^{2+}]$ in the pipette was 20 nM, measured using fura-2 as described previously (Grynkiewicz *et al.*, 1985). Perforated-patch experiments (Horn and Marty, 1988) were conducted with a pipette solution containing (in mM) 55 KCl, 70 K_2SO_4, 7 $MgCl_2$, 5 D-glucose, and 10 K-HEPES (pH 7.2), with 200 μg/ml nystatin (Sigma Chemical Co., St. Louis, MO). In all experiments, an Axopatch 1B (Axon Instruments) patch-clamp

amplifier was used in the voltage-clamp mode, and the output was filtered at 2 kHz with an 8-pole Bessel filter (Frequency Devices, Haverhill, MA). Stimulation and recording was done with a PDP computer and interface (Indec Systems, Sunnyvale, CA). In voltage-ramp experiments, the holding potential was −60 mV; ramp data were corrected for linear leakage and capacitive current recorded between −80 and −40 mV immediately after break-in and were filtered off-line at 300 Hz using a digital Gaussian filter algorithm. Command voltage was corrected for liquid junction potentials between pipette and bath in whole-cell and perforated-patch experiments (−13 and −10 mV, respectively).

Jurkat cells, loaded with fura-2 as described above, were illuminated using a Zeiss 100-W Hg arc lamp (attenuated 200-fold) and 350- and 385-nm interference filters (bandwidths = 10 nm). Emitted fluorescence at 500 nm (100-nm bandwidth) was collected through a pinhole equal to the cell diameter, with a photomultiplier tube (Model 647-04, Hamamatsu) and photon-counting photometer (Model 126, Pacific Instruments, Concord, CA). A 63× oil-immersion lens was used (Zeiss Neofluar, N.A. 1.25). To avoid dye bleaching, an electronic shutter restricted the illumination to a 50-ms period every 1–2 s. Photomultiplier output was sampled and processed online using the patch-clamp interface described above.

Calibration of cellular fura-2 signals

Attempts to calibrate cellular fura-2 signals using fura-2 in free solution (K aspartate solution with either 10 mM EGTA or 10 mM $CaCl_2$) yielded inaccurate results, often producing estimates of cellular $[Ca^{2+}]_i$ less than zero. This problem results from changes in the properties of fura-2 brought about by the intracellular environment (Almers and Neher, 1985; Malgaroli *et al.*, 1987; Konishi *et al.*, 1988). Therefore, all calibrations were performed with dye-loaded cells according to the patch-pipette method of Almers and Neher (1985). Cells were loaded with fura-2/AM as described above, then plated onto coverslips treated with poly-D-lysine (0.2–0.5 mg/ml; Sigma). R_{min} was measured as the R value following break-in with a pipette solution of K aspartate and 10 mM EGTA. R_{max} was determined as the R value after break-in with K aspartate and 10 mM $CaCl_2$ or as the R value of intact cells incubated in 5 μM ionomycin and Ringer solution containing 10 mM $CaCl_2$. K^* was determined after break-in with a K aspartate solution containing 30 mM EGTA and 180 nM free Ca^{2+}.

Acknowledgments

We are grateful to Mr. Paul Steinbach for help in setting up the video imaging system, for writing image acquisition and analysis programs, and for stimulating discussions throughout the course of this work. We are also indebted to Dr. Stephan Grissmer for help with the perforated-patch technique, Ms. Ruth Davis for technical assistance and cell culture, and Dr. Erwin Neher for thoughtful comments on the manuscript. This work was supported by NIH grants GM-41514 and NS-14609 and by the Office of Naval Research.

Received: July 31, 1989.

References

Almers, W., and Neher, E. (1985). The Ca signal from fura-2 loaded mast cells depends strongly on the method of dye-loading. FEBS Lett. *192,* 13–18.

Ambler, S.K., Poenie, M., Tsien, R.Y., and Taylor, P. (1988). Agonist-stimulated oscillations and cycling of intracellular free calcium in individual cultured muscle cells. J. Biol. Chem. *263,* 1952–1959.

Berridge, M.J., Cobbold, P.H., and Cuthbertson, K.S.R. (1988). Spatial and temporal aspects of cell signalling. Philos. Trans. R. Soc. Lond. B Biol. Sci. *320,* 325–343.

Berridge, M.J., and Irvine, R.F. (1984). Inositol trisphosphate, a novel second messenger in cellular signal transduction. Nature *312,* 315–321.

Bijsterbosch, M.K., Rigley, K.P., and Klaus, G.G.B. (1986). Cross-linking of surface immunoglobulin on B lymphocytes induces both intracellular Ca^{2+} release and Ca^{2+} influx: analysis with indo-1. Biochem. Biophys. Res. Commun. *137,* 500–506.

Cahalan, M.D., Chandy, K.G., DeCoursey, T.E., and Gupta, S. (1985). A voltage-gated potassium channel in human T lymphocytes. J. Physiol. *358,* 197–237.

Cuthbertson, K.S.R., and Cobbold, P.H. (1985). Phorbol ester and sperm activate mouse oocytes by inducing sustained oscillations in cell Ca^{2+}. Nature *316,* 541–542.

DeCoursey, T.E., Chandy, K.G., Gupta, S., and Cahalan, M.D. (1984). Voltage-gated K^+ channels in human T lymphocytes: a role in mitogenesis? Nature *307,* 465–468.

Fukushima, Y., Hagiwara, S., and Henkart, M. (1984). Potassium current in clonal cytotoxic T lymphocytes from the mouse. J. Physiol. *351,* 645–656.

Gardner, P., Alcover, A., Kuno, M., Moingeon, P., Weyand, C.M., Goronzy, J., and Reinherz, E.L. (1989). Triggering of T-lymphocytes via either T3-Ti or T11 surface structures opens a voltage-insensitive plasma membrane calcium-permeable channel: requirement for interleukin-2 gene function. J. Biol. Chem. *264,* 1068–1076.

Gelfand, E.W., Cheung, R.K., and Grinstein, S. (1984). Role of membrane potential in the regulation of lectin-induced calcium uptake. J. Cell. Physiol. *121,* 533–539.

Gelfand, E.W., Cheung, R.K., Grinstein, S., and Mills, G.B. (1986). Characterization of the role for calcium influx in mitogen-induced triggering of human T cells. Identification of calcium-dependent and calcium-independent signals. Eur. J. Immunol. *16,* 907–912.

Gray, L.S., Gnarra, J.R., Sullivan, J.A., Mandell, G.L., and Engelhard, V.H. (1988). Spatial and temporal characteristics of the increase in intracellular Ca^{2+} induced in cytotoxic T lymphocytes by cellular antigen. J. Immunol. *141,* 2424–2430.

Grissmer, S., and Cahalan, M. (1989). Ionomycin activates a potassium-selective conductance in human T lymphocytes. Biophys. J. *55,* 245a.

Grynkiewicz, G., Poenie, M., and Tsien, R.Y. (1985). A new generation of Ca^{2+} indicators with greatly improved fluorescence properties. J. Biol. Chem. *260,* 3440–3450.

Hagiwara, S., and Byerly, L. (1981). Calcium channel. Annu. Rev. Neurosci. *4,* 69–125.

Hallam, T.J., and Rink, T.J. (1985). Agonists stimulate divalent cation channels in the plasma membrane of human platelets. FEBS Lett. *186,* 175–179.

Hamill, O.P., Marty, A., Neher, E., Sakmann, B., and Sigworth, F.J. (1981). Improved patch-clamp techniques for high-resolution current recording from cells and cell-free membrane patches. Pfluegers Arch. *391,* 85–100.

Hesketh, T.R., Moore, J.P., Morris, J.D.H., Taylor, M.V., Rogers, J., Smith, G.A., and Metcalfe, J.C. (1985). A common sequence of calcium and pH signals in the mitogenic stimulation of eukaryotic cells. Nature *313,* 481–484.

Horn, R., and Marty, A. (1988). Muscarinic activation of ionic currents measured by a new whole-cell recording method. J. Gen. Physiol. *92,* 145–159.

Imboden, J.B., and Stobo, J.D. (1985). Transmembrane signalling by the T cell antigen receptor. J. Exp. Med. *161,* 446–456.

Imboden, J.B., and Weiss, A. (1987). The T-cell antigen receptor regulates sustained increases in cytoplasmic free Ca^{2+} through extracellular Ca^{2+} influx and ongoing intracellular Ca^{2+} mobilization. Biochem. J. *247,* 695–700.

Ishida, Y., and Chused, T.M. (1988). Heterogeneity of lymphocyte calcium metabolism is caused by T cell-specific calcium-sensitive potassium channel and sensitivity of the calcium ATPase pump to membrane potential. J. Exp. Med. *168,* 839–852.

Jacob, R., Merritt, J.E., Hallam, T.J., and Rink, T.J. (1988). Repetitive spikes in cytoplasmic calcium evoked by histamine in human endothelial cells. Nature *335,* 40–45.

June, C.H., Ledbetter, J.A., Rabinovitch, P.S., Martin, P.J., Beatty, P.G., and Hansen, J.A. (1986). Distinct patterns of transmembrane calcium flux and intracellular calcium mobilization after differentiation antigen cluster 2 (E rosette receptor) or 3 (T3) stimulation of human lymphocytes. J. Clin. Invest. *77,* 1224–1232.

Kanner, B.I., and Metzger, H. (1984). Initial characterization of the calcium channel activated by the cross-linking of the receptors for immunoglobulin E. J. Biol. Chem. *259,* 10188–10193.

Konishi, M., Olson, A., Hollingworth, S., and Baylor, S.M. (1988). Myoplasmic binding of fura-2 investigated by steady-state fluorescence and absorbance measurements. Biophys. J. *54,* 1089–1104.

Kuno, M., and Gardner, P. (1987). Ion channels activated by inositol 1,4,5-trisphosphate in plasma membrane of human T-lymphocytes. Nature *326,* 301–304.

Kuno, M., Goronzy, J., Weyand, C.M., and Gardner, P. (1986). Single-channel and whole-cell recordings of mitogen-regulated inward currents in human cloned helper T lymphocytes. Nature *323,* 269–273.

Lewis, R.S., and Cahalan, M.D. (1989). Ion channels and calcium signaling in single mitogen-stimulated T lymphocytes. In: Immunogenicity, UCLA Symposia on Molecular and Cellular Biology, New Series, Vol. 113, eds. C. Janeway, J. Sprent, and E. Sercarz, New York: Alan R. Liss, Inc. (in press)

Llano, I., Marty, A., and Tanguy, J. (1987). Dependence of intracellular effects of GTPγS and inositoltrisphosphate on cell membrane potential and on external Ca ions. Pfluegers Arch. *409,* 499–506.

MacDonald, H.R., and Nabholz, M. (1986). T-cell activation. Annu. Rev. Cell Biol. *2,* 231–253.

MacDougall, S.L., Grinstein, S., and Gelfand, E.W. (1988). Detection of ligand-activated conductive Ca^{2+} channels in human B lymphocytes. Cell *54,* 229–234.

Malgaroli, A., Milani, D., Meldolesi, J., and Pozzan, T. (1987). Fura-2 measurement of cytosolic free Ca^{2+} in monolayers and suspensions of various types of animal cells. J. Cell Biol. *105,* 2145–2155.

Mastro, A.M., and Smith, M.C. (1983). Calcium-dependent activation of lymphocytes by ionophore, A23187, and a phorbol ester tumor promoter. J. Cell. Physiol. *116,* 51–56.

Matteson, D.R., and Deutsch, C. (1984). K channels in T lymphocytes: a patch clamp study using monoclonal antibody adhesion. Nature *307,* 468–471.

Matthews, G., Neher, E., and Penner, R. (1989). Second messenger-activated calcium influx in rat peritoneal mast cells. J. Physiol. (in press)

Merritt, J.E., and Rink, T.J. (1987). Regulation of cytosolic free calcium in fura-2-loaded rat parotid acinar cells. J. Biol. Chem. *262,* 17362–17369.

Meyer, T., Holowka, D., and Stryer, L. (1988). Highly cooperative opening of calcium channels by inositol 1,4,5-trisphosphate. Science *240,* 653–656.

Meyer, T., and Stryer, L. (1988). Molecular model for receptor-stimulated calcium spiking. Proc. Natl. Acad. Sci. USA *85,* 5051–5055.

Miyazaki, S., Hashimoto, N., Yoshimoto, Y., Kishimoto, T., Igusa, Y., and Hiramoto, Y. (1986). Temporal and spatial dynamics of the periodic increase in intracellular free calcium at fertilization of golden hamster eggs. Dev. Biol. *118,* 259–267.

Neher, E., and Almers, W. (1986). Fast calcium transients in rat peritoneal mast cells are not sufficient to trigger exocytosis. EMBO J. *5,* 51–53.

Nisbet-Brown, E., Cheung, R.K., Lee, J.W.W., and Gelfand, E.W. (1985). Antigen-dependent increase in cytosolic free calcium in specific human T-lymphocyte clones. Nature *316,* 545–547.

Oettgen, H.C., Terhorst, C., Cantley, L.C., and Rosoff, P.M. (1985). Stimulation of the T3-T cell receptor complex induces a membrane-potential-sensitive calcium influx. Cell *40,* 583–590.

Payne, R., Walz, B., Levy, S., and Fein, A. (1988). The localization of calcium release by inositol trisphosphate in *Limulus* photoreceptors and its control by negative feedback. Philos. Trans. R. Soc. Lond. B Biol. Sci. *320,* 359–379.

Penner, R., Matthews, G., and Neher, E. (1988). Regulation of calcium influx by second messengers in rat mast cells. Nature *334,* 499–504.

Putney, J.W., Jr. (1986). A model for receptor-regulated calcium entry. Cell Calcium *7,* 1–12.

Schlichter, L.C., and Mahaut-Smith, M.P. (1989). Ca^{2+}-activated K channels in B and T lymphocytes. Biophys. J. *55,* 6a.

Streb, H., Irvine, R.F., Berridge, M.J., and Schulz, I. (1983). Release of Ca^{2+} from a nonmitochondrial intracellular store in pancreatic acinar cells by inositol-1,4,5-trisphosphate. Nature *306,* 67–69.

Supattapone, S., Worley, P.F., Baraban, J.M., and Snyder, S.H. (1988). Solubilization, purification, and characterization of an inositol trisphosphate receptor. J. Biol. Chem. *263,* 1530–1534.

Treves, S., Di Virgilio, F., Cerundolo, V., Zanovello, P., Collavo, D., and Pozzan, T. (1987). Calcium and inositolphosphates in the activation of T cell-mediated cytotoxicity. J. Exp. Med. *166,* 33–42.

Truneh, A., Albert, F., Golstein, P., and Schmitt-Verhulst, A.-M. (1985). Early steps of lymphocyte activation bypassed

by synergy between calcium ionophores and phorbol ester. Nature *313,* 318–320.

Tsien, R.Y., Pozzan, T., and Rink, T.J. (1982). T-cell mitogens cause early changes in cytoplasmic free Ca^{2+} and membrane potential in lymphocytes. Nature *295,* 68–71.

von Tscharner, V., Prod'hom, B., Baggiolini, M., and Reuter, H. (1986). Ion channels in human neutrophils activated by a rise in free cytosolic calcium concentration. Nature *324,* 369–372.

Weiss, A., and Imboden, J.B. (1987). Cell surface molecules and early events involved in human T lymphocyte activation. Adv. Immunol. *41,* 1–38.

Weiss, A., Imboden, J., Shoback, D., and Stobo, J. (1984). Role of T3 surface molecules in human T-cell activation: T3-dependent activation results in an increase in cytoplasmic free calcium. Proc. Natl. Acad. Sci. USA *81,* 4169–4173.

Weiss, M.J., Daley, J.F., Hodgdon, J.C., and Reinherz, E.L. (1984). Calcium dependency of antigen-specific (T3-Ti) and alternative (T11) pathways of human T-cell activation. Proc. Natl. Acad. Sci. USA *81,* 6836–6840.

Whitney, R.B., and Sutherland, R.M. (1972). Requirement for calcium ions in lymphocyte transformation stimulated by phytohemagglutinin. J. Cell. Physiol. *80,* 329–338.

Williamson, J.R., Cooper, R.H., Joseph, S.K., and Thomas, A.P. (1985). Inositol trisphosphate and diacylglycerol as intracellular second messengers in liver. Am. J. Physiol. *248,* C203–C216.

Wilson, H.A., Greenblatt, D., Poenie, M., Finkelman, F.D., and Tsien, R.Y. (1987). Crosslinkage of B lymphocyte surface immunoglobulin by anti-Ig or antigen induces prolonged oscillations of intracellular ionized calcium. J. Exp. Med. *166,* 601–606.

Woods, N.M., Cuthbertson, K.S.R., and Cobbold, P.H. (1987). Agonist-induced oscillations in cytoplasmic free calcium concentration in single rat hepatocytes. Cell Calcium *8,* 79–100.

Zschauer, A., van Breemen, C., Buehler, F.R., and Nelson, M.T. (1988). Calcium channels in thrombin-activated human platelet membrane. Nature *334,* 703–705.